*13th Australasian Fluid Mechanics Conference*
*Monash University, Melbourne, Australia*
*13-18 December 1998*

# *Flow pattern detection in a gas-liquid reactor by gas supply line pressure fluctuation measurements*

J.J.J. Chen, J.C. Zhao and Z.D. Chen

School of Engineering
The University of Auckland,
Private Bag 92019, Auckland,
New Zealand

## *Abstract*

In a stirred gas-liquid reactor, four flow patterns are generally recognized: *flooding*, *minimum dispersion*, *intimate dispersion* and *uniform dispersion*. To achieve good bubble dispersion and high mass transfer, the well dispersed flow pattern, *i.e. intimate* or *uniform dispersion,* is most desirable, while the inferior dispersion pattern, *i.e. flooding* or *minimum dispersion*, should be avoided.

In this paper, a non-intrusive measurement method is reported for a gas-liquid reactor using a Rushton impeller which is commonly used in chemical and biochemical processes. It involves measuring the pressure fluctuations in the gas supply line leading to the gas sparger, analyzing the power spectra in the frequency domain, and extracting useful information from the fluctuating signals. It is shown that the information extracted may be related to the flow patterns observed.

## *Introduction*

Two-phase gas-liquid reactors with mechanical agitation are widely used for mixing, chemical reaction, fermentation, mineral flotation and metallurgical processes. Four flow patterns are generally recognized within the gas-liquid mixture[1]. These are *flooding (F)*, *minimum dispersion (MD)*, *intimate dispersion (ID)* and *uniform dispersion (UD)*. To achieve good bubble dispersion and high mass transfer, the well dispersed flow pattern, *i.e. intimate* or *uniform dispersion,* is most desirable; while the inferior dispersion pattern, *i.e. flooding* or *minimum dispersion*, should be avoided.

Flow patterns have been studied by a number of workers. Hsi *et al*[2], and Sutter *et al*[3] measured the sound spectra in an agitated tank using a hydrophone, and related the spectra to the gas dispersions. Warmoeskerken & Smith[4] analysed the gas dispersion pattern based on the gassed power measurement and cavity formation observations in a stirred tank using a disc-turbine. Chen & Zhao[5] studied flow patterns in terms of a balance of the radial and buoyancy forces that prevail near the stirrer. Zhao[6], Walker *et al*[7],and Zhao & Chen[8] investigated the flow pattern by measuring local pressure fluctuations at points situated within the gas-liquid mixture. Zhao[6], and Chen *et al*[9] also related the gas dispersion pattern to a parameter derived from the pressure fluctuations measured on the gas supply line which is connected to a hollow shaft in a molten metal treatment water model. However, some of these methods are intrusive, and others are restricted to particular designs of the equipment.

Generally, gas is introduced into the gas-liquid reactor via a ring sparger situated below the stirrer. The pressure within the supply line will fluctuate, and the characteristics of the fluctuations may vary with various gas flow rate and are also affected by the interaction forces between the gas flow and the liquid. The strength and characteristics of the interaction forces are affected by the dispersion behaviours of the impeller. In other words, the pressure fluctuation in the gas supply line is affected by the gas flow rate and the impeller speed, and may be related to the gas dispersion patterns.

In this paper, a non-intrusive measurement method is reported for a gas-liquid reactor using a Rushton impeller. It involves measuring the pressure fluctuations in the gas supply line leading to the gas sparger, analyzing the power spectra in the frequency domain, and extracting useful information from the fluctuating signals. It will be shown that the information extracted may be related to the flow pattern observed.

## *Experimental set-up*

The experimental set-up is shown schematically in Fig. 1. A flat-bottom cylindrical vessel fitted with four vertical wall baffles was made of transparent Plexiglass with an internal diameter $T$=0.19m. Tap water was used in the experiments and the liquid height was kept the same as the vessel diameter. A Rushton impeller was used as the agitator. The impeller was located $T/3$ above the base. The diameter of the impeller was $D=T/3$.

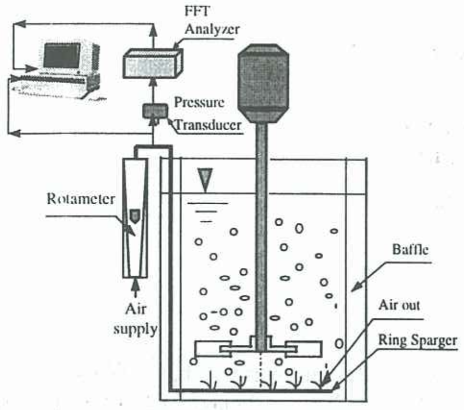


Fig. 1. Schematic view of the experimental system

The air was introduced into the reactor by a ring-sparger located at the bottom of the tank, and it has the same diameter as the impeller. Typical dimensions of the experimental system and the impeller used are listed in Table 1.

| Vessel | dimension | Impeller | dimension |
|---|---|---|---|
| T(m) | 0.19 | D(m) | T/3 |
| B(m) | T/10 | d(m) | 0.75D |
| H(m) | T | W(m) | 0.2D |
| C(m) | T/3 | A($m^2$) | 0.2Dx0.25D |
| S(m) | T/3 | Bt(mm) | 1.5 |

Table 1. Typical dimensions

A pressure transducer with a measurement range of 0-1 psi (0-6.9kPa) was installed on the gas supply line leading to the ring-sparger. The pressure fluctuations were processed in the frequency domain in the form of power spectra using a FFT analyzer (Model: Rockland 5840A).

## *Results*

Experiments were conducted at the air flow rate (*Q*) range of 2.5 to 20 *litres/min*( STP ) with increments of 2.5 *litres/min*, and the impeller speed (*n*) ranged from 0 to 1000 *rpm*. The frequency range of the measurement was 0-500Hz, and the average power spectra were obtained.

The gas-liquid flow patterns were also visually observed and recorded. A series of photographs taken at various combinations of the air flow rate and impeller speed were arranged in a matrix according to the operating conditions as shown in Fig. 2, and served as the basis for the gas dispersion pattern comparison. At a given air flow rate, the flow pattern varied with increasing impeller speed, changing from the inferior dispersion to the well-dispersed, and this occurs at a certain impeller speed for a given fixed air flow rate.

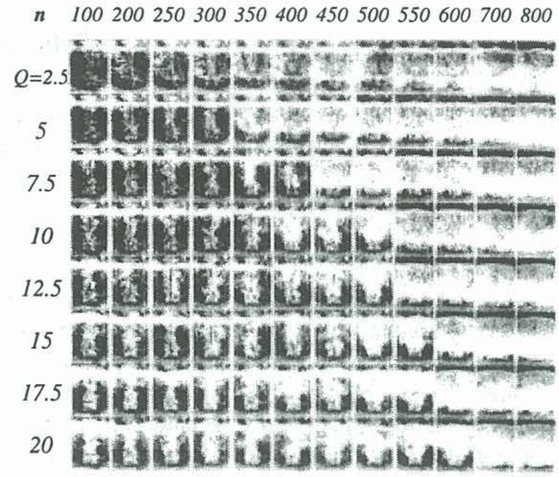


Fig. 2. Flow pattern observed in a Rushton water model

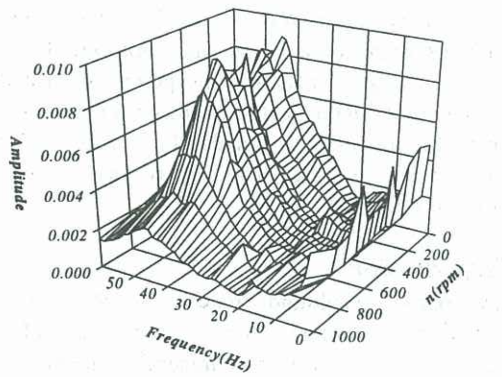


Fig. 3. Power spectra vs the impeller speed at an air flow rate of 10 *litres/min*

Typical average power spectra in the frequency range of 0-60Hz are shown in Fig. 3. The spectra were obtained at a fixed air flow rate of 10 *litres/min* and at various impeller speeds ranging from 0 to 1000 *rpm* as indicated on the figure. It can be seen that at a fixed air flow rate, the strength of the power varies with the impeller speed. Within the impeller speed range of 0 to 450 *rpm*, the power spectra remain almost unchanged with the impeller speed. However, beyond an impeller speed of 450 *rpm*, with a further increase in the impeller speed, there is a considerable increase in the strength of the power spectra in the frequency range of 30-60Hz. Beyond an impeller speed of 600 *rpm*, the strength of the power spectra in the frequency range of 30-60Hz reduces with a further increase in the impeller speed. When the characteristics of the power spectra shown in Fig. 3 are compared with the flow patterns as shown in Fig. 2, it is clear that there is a direct correlation.

To characterise the power spectra, a quantitative parameter needs to be found. From an analysis of the power spectra, various parameters were defined and parameters in various frequency ranges were examined. One of the parameters considered was found to exhibit some very interesting characteristic features, and the variation of the parameter may be related to the flow pattern transition. In this paper, this parameter will be defined as the Ratio of the Power (*ROP*) within the frequency range of 0-30*Hz* to that in the frequency range of 0-60*Hz*. Its value was calculated using the trapezium rule as shown in Eq. 1:

$$ROP = \frac{\int_0^{30} p(f)df}{\int_0^{60} p(f)df} \approx \frac{\sum_{i=0}^{k1} p_i - (p_0 + p_{k1})/2}{\sum_{i=0}^{k2} p_i - (p_0 + p_{k2})/2} \quad (1)$$

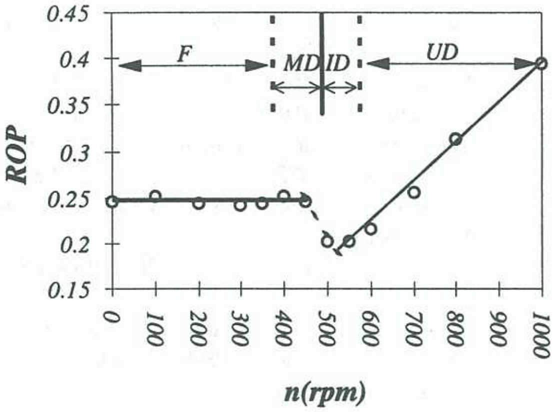


Fig. 4. *ROP* calculated from the power spectra shown in Fig. 3.

Using the spectra such as those shown in Fig. 3 for Q=10 *litres/min*, the *ROP* values were calculated and plotted against the impeller speed (*n*) as shown in Fig. 4. In the same figure, the flow patterns are also indicated. It can be seen that there is a direct correlation between the flow pattern and *ROP*.

The *ROP* values obtained at other air flow rates and impeller speeds are plotted in a 3-D manner as shown in Fig. 5. There is clearly a rather complex relationship between the *ROP*, *n* and *Q*. Generally, at a fixed air flow rate, the *ROP* varies with the impeller speed. However, over a certain range of low impeller speeds, *ROP* remains unchanged with the impeller speed. Then, beyond a certain impeller speed, a sudden drop in the value of *ROP* occurred with a further increase in the impeller speed. Beyond this maxima, the *ROP* increases gradually with a further increase in the impeller speed. The critical impeller speed at which the sudden drop in the *ROP* value occurs varies depending on the air flow rate. This critical impeller speed is high when the air flow rate is high, and low when the air flow rate is low.

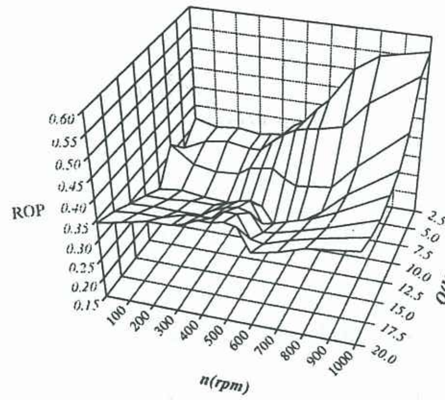


Fig. 4. 3-D view of the *ROP*

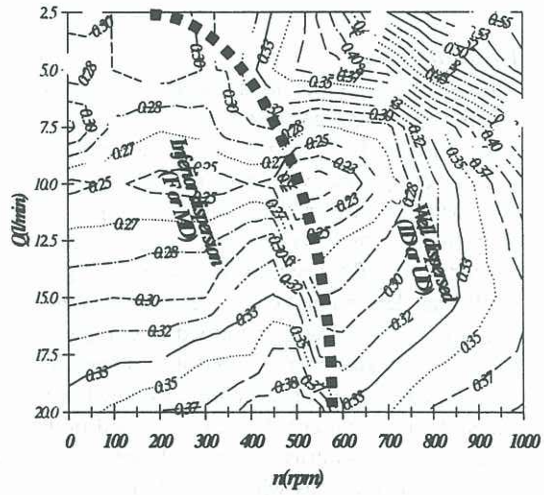


Fig. 6. 2-D contour of the *ROP*

The variation of the *ROP* value with the impeller speed and the air flow rate is also shown in Fig. 6, which is a 2-D contour plot. On this figure, a boundary ( dashed-line ) was drawn to separate the *well dispersed* and the *inferior dispersion* flow regimes. This line lies on the bottom of the "valley" as shown in Fig. 5. The *inferior dispersion* regime is located in a zone on the lower left-side of the line, while the *well dispersed* is situated in a zone on the upper right-side of the line. This may be further confirmed if a comparison between Fig.2 and Fig.6 is made.

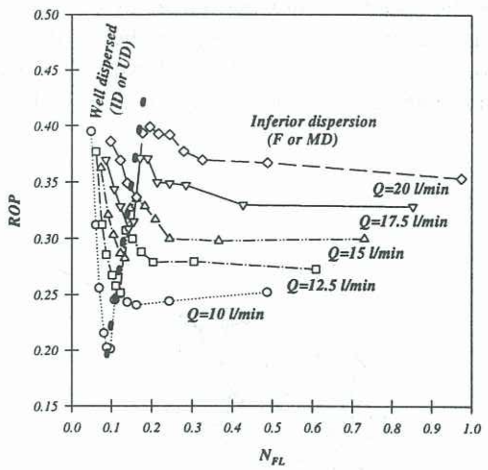


Fig. 7. *ROP* vs the Air flow number

The air flow number given as $N_{Fl}$ ( $Q/nD^3$ ) may also be used as a correlation parameter. Fig. 7 shows a plot of the *ROP* value vs the air flow number. A family of curves with a very distinct shape results. A dashed-line had been included in Fig. 7 to separate the *ID* or *UD* from *F* or *MD*.

## Conclusions

The pressure fluctuations on the gas supply line leading to the sparger of a gas-liquid agitated reactor were measured at various operating conditions, and the power spectra were obtained. It was found that the power spectra in the frequency range of 0-60Hz showed certain characteristic features which are related to the flow pattern transitions. A parameter, *ROP*, was defined and calculated based on the power spectra. The *ROP* was examined in comparison with the flow pattern observed, and it was shown that the flow pattern observed may be correlated with *ROP*. Thus, the flow pattern delineation based on the *ROP* provides a non-intrusive method for flow pattern detection in situations where direct visual observation is impossible or impractical.

## Acknowledgment

The Foundation of Research Science Technology of New Zealand provided support for this work.

## List of symbols

A. Blade projected area, $m^2$.
B. Width of the wall baffles(x4), *m*.
Bt. Blade thickness, *m*.
C. Clearance of impeller, *m*.
D. Impeller diameter, *m*.
d. Diameter of disk, *m*.
H. Liquid height, *m*.
S. Diameter of ring sparger, *m*.
T. Tank internal diameter, *m*.
W. Width of blade, *m*.
*n*. Impeller speed, *rpm*.
*Q*. Air flow rate, *litres/min*.
$N_{Fl}$ Air flow number, $Q/nD^3$, dimensionless.

## References

1. Oldshue, J. Y., 1983, Fluid Mixing Technology, (*Chemical Engineering*), McGraw-Hill.
2. Hsi, R., Tay, M., Bukur, D., Tatterson, G. & Morrison, G., 1985, "Sound spectra of gas dispersion in an agitated tank", *The Chem. Eng. Journal*, **31**, 153-161.
3. Sutter, T. A., Morrison, G. L. & Tatterson, G. B., 1987, "Sound spectra in an aerated agitated tank", *AIChE*, **33**(44), 668-671.
4. Warmoeskerken, M. M. C. G. & Smith, J. M., 1985, "Flooding of Disc Turbines in Gas-liquid Dispersion: A New Description of the Phenomena", *Chem. Eng. Sci.*, **40**, 2063-2071.
5. Chen, J. J. J. & Zhao J. C., 1995, "Bubble Distribution in a Melt Treatment Water Model", *Light Metals*, 1227-1231.
6. Zhao J. C., 1997, "Molten Aluminium Treatment Model Studies", ***PhD Thesis***, The University of Auckland, October.
7. Walker M. L., Zhao J. C. & Chen J. J. J., 1995, "Bubble Flow Pattern Detection in the Water Model of a Metal Treatment Unit", ***Proceedings of the 1995 PACRIM Congress***, The Australia Institute of Mining and Metallurgy, 19-22 November, 605-609.
8. Zhao J. C. & Chen J. J. J., 1998, "Flow Pattern Detection Using Pressure Fluctuation Measurements within a Gas-liquid Reactor", *IPENZ* Conference 1998, Auckland, New Zealand, 12-15 February.
9. Chen J. J. J., Zhao J. C. & Chen Z. D., 1998, "Flow Pattern Detection in a Metal Treatment Water Model by On-line Pressure Fluctuation Measurements", ***International Conference on Mixing and Crystallisation***, Tioman Island, Malaysia, 22-25 April.